











ORIGINAL RESEARCH

 OPEN ACCESS



Lymphatic vessel density is associated with CD8⁺ T cell infiltration and immunosuppressive factors in human melanoma

Natacha Bordry ^{a,b,*}, Maria A. S. Broggi ^{b,h,*}, Kaat de Jonge ^a, Karin Schaeuble^a, Philippe O. Gannon^c, Periklis G. Foukas^{c,g}, Esther Danenberg^c, Emanuela Romano^{c,e}, Petra Baumgaertner^{a,c}, Manuel Fankhauser ^b, Noémie Wald^a, Laurène Cagnon^c, Samia Abed-Maillard ^c, Hélène Maby-El Hajjami ^a, Timothy Murray^a, Kalliopi Ioannidou ^a, Igor Letovanec ^d, Pu Yan^d, Olivier Michielin^c, Maurice Matter ^{c,g}, Melody A. Swartz^{b,f}, and Daniel E. Speiser ^{a,c}

^aClinical Tumor Biology and Immunotherapy Group, Department of Oncology and Ludwig Cancer Research, University of Lausanne (UNIL), Lausanne, Switzerland; ^bInstitute of Bioengineering and Swiss Institute for Experimental Cancer Research (ISREC), School of Life Sciences, Ecole Polytechnique Fédérale de Lausanne, Lausanne, Switzerland; ^cDepartment of Oncology, Lausanne University Hospital Center (CHUV) and University of Lausanne, Lausanne, Switzerland; ^dDepartment of Pathology, CHUV, Lausanne, Switzerland; ^eDepartment of Oncology, INSERM U932, Institut Curie, Paris, FRANCE; ^f2nd Department of Pathology, Attikon University Hospital, National and Kapodistrian University of Athens, Athens, Greece; ^gDepartment of Surgery, CHUV, Lausanne, Switzerland; ^hInstitute for Molecular Engineering, University of Chicago, Chicago, IL, USA

ABSTRACT

Increased density of tumor-associated lymphatic vessels correlates with poor patient survival in melanoma and other cancers, yet lymphatic drainage is essential for initiating an immune response. Here we asked whether and how lymphatic vessel density (LVD) correlates with immune cell infiltration in primary tumors and lymph nodes (LNs) from patients with cutaneous melanoma. Using immunohistochemistry and quantitative image analysis, we found significant positive correlations between LVD and CD8⁺ T cell infiltration as well as expression of the immunosuppressive molecules inducible nitric oxide synthase (iNOS) and 2,3-dioxygenase (IDO). Interestingly, similar associations were seen in tumor-free LNs adjacent to metastatic ones, indicating loco-regional effects of tumors. Our data suggest that lymphatic vessels play multiple roles at tumor sites and LNs, promoting both T cell infiltration and adaptive immunosuppressive mechanisms. Lymph vessel associated T cell infiltration may increase immunotherapy success rates provided that the treatment overcomes adaptive immune resistance.

ARTICLE HISTORY

Received 16 November 2017
Revised 25 February 2018
Accepted 13 March 2018

KEYWORDS

Immunotherapy; lymphatics; tumor immunology; T cell inhibition; T cell promotion


Introduction

Over the last two decades, burgeoning research attention has been focused on understanding the complex interactions between evolving tumors and host immune responses, with consequences for the development of novel immunotherapies.¹⁻⁴ Despite the promotion of tumor antigen specific T cell responses by active immunization, checkpoint blockade or adoptive transfer, only a subset of patients experience clinical benefit.⁵ In melanoma, recent studies have sought predictive indicators (genetic or phenotypic) by comparing patients who respond to immunotherapies with those that do not.^{6,7} A variety of factors have been found to affect response to immunotherapy, including the preexisting immune cell infiltrate and the chemokine expression profile.^{8,9} Furthermore, cancers can develop adaptive immune resistance mechanisms that suppress anti-tumor T cell responses.^{10,11} In addition, further mechanisms may contribute to therapy failures, including mechanisms that impact on the recruitment of immune cells to tumors.¹² New and readily accessible/quantifiable biomarkers are

required to help identifying the underlying reasons in individual patients, and consequently adapt immune therapy strategies in order to increase patient survival.¹³

One feature of many cancers is the activation or expansion of lymphatic vessels. Local lymphatic vessel density (LVD) is known to be associated with metastasis in several human and experimental cancers. The lymphangiogenic factor Vascular Endothelial Growth Factor-C (VEGF-C), secreted by tumor-associated macrophages or tumor cells themselves, leads to increased LVD in the tumor microenvironment and in lymph nodes (LNs), correlating with increased metastasis and poor prognosis.¹⁴⁻²⁰ However, the mechanisms by which lymphangiogenesis promotes disease progression are not well understood. While increased LVD provide more surface area for tumor cells to enter the lymph and thereby migrate to distant sites, recent studies have highlighted additional important mechanisms. For example, VEGF-C activates lymphatic endothelial cells (LECs) to upregulate chemokine (C-C motif) ligand 21 (CCL21), a chemo-attractant for C-C chemokine receptor

CONTACT Daniel E. Speiser  doc@dspeiser.ch; Melody A. Swartz  melodyswartz@uchicago.edu

 Supplemental data for this article can be accessed on the [publisher's website](#).

*These authors contributed equally to this article.

© 2018 The Author(s). Published with Taylor & Francis Group.

This is an Open Access article distributed under the terms of the Creative Commons Attribution-NonCommercial-NoDerivatives License (<http://creativecommons.org/licenses/by-nc-nd/4.0/>), which permits non-commercial re-use, distribution, and reproduction in any medium, provided the original work is properly cited, and is not altered, transformed, or built upon in any way.

7⁺ (CCR7) immune cells and tumor cells, leading to increased tumor invasion and entry into lymphatics *in vitro* and *in mice*.²¹⁻²³ More recently, it has been proposed that lymphangiogenesis could play important roles in modulating the immune microenvironment. In mouse models, increased CCL21 in the tumor microenvironment could promote fibroblast differentiation and matrix remodeling to resemble the stroma of lymph nodes, as well as promote T cell infiltration (including regulatory T cells) along with suppressive leukocyte subsets.²⁴ Furthermore, tumor-associated LECs may directly cross-present tumor antigens to CD8⁺ T cells and render them dysfunctional in the tumor microenvironment.^{25,26} LECs can also inhibit the maturation of dendritic cells,²⁷ secrete inhibitory molecules such as indoleamine 2,3-dioxygenase (IDO), inducible nitric oxide synthase (iNOS) and transforming growth factor beta (TGF- β), and impair T cell activation through expression of inhibitory receptor ligands (e.g. programmed cell death ligand 1 and 2 (PD-L1 and 2)).²⁸ Finally, a recent study demonstrated that in mice lacking dermal lymphatic vessels, melanomas failed to generate an inflammatory microenvironment and lacked T cell infiltration.²⁹ Taken together, these findings indicate a critical role for tumor-associated lymphatics in initiating and shaping the immune response.

Since these studies were performed in mice, in short-term studies with implanted tumors, we asked whether and how LVD correlates with the immune microenvironment in patients with cutaneous melanoma. Through immunohistochemistry (IHC) analysis of primary tumors and downstream LNs, using a dedicated method enabling quantitative assessment of unusually large tissue fields, we provide evidence that LVD indeed correlates with T cell infiltration and expression of immune suppressive molecules in human melanoma, not only locally but also in regional LNs, including in those that are not (yet) metastatic. Our findings suggest that while LVD and VEGF-C are prognostic factors for metastasis, they also are tightly correlated with the immune status of the tumor microenvironment and thus may have potential impact on the outcome of immunotherapy.

Results

Quantification of lymph vessels across entire tissue sections

To determine LVD we examined LECs by IHC staining in sections of tumors and draining LNs. We found high variability of LVD in different regions of the tumor, as well as high inter-patient heterogeneity. Thus, we first sought to establish a method of analyzing entire tumor sections for very wide and representative spatial assessment of LVD and related features of the immune microenvironment. We defined distinct tissue zones in the tumor and LN microenvironments to study 13 primary tumors, 23 metastatic LNs and 23 tumor-free LNs (i.e. neighboring distant lymph node without evidence of disease) and used whole-slide imaging software for quantifications in each zone (see Methods).

To define the localization of LECs in different human tissue sections we performed IHC using Prox-1 and podoplanin antibodies. Histological analysis confirmed that

podoplanin was specifically expressed on lymphatic vessels in different zones of the primary tumor (Fig. 1A), the tumor region of metastatic LNs (Fig. 1B) and the normal skin (Fig. S1A). In contrast, Prox-1 antibody was not well suited as LEC marker within these tissues, as certain tumor cells as well as skin epithelial cells may also be positive (Fig. 1A and B and Fig. S1A and B).

Up to now, histological quantification of human lymphatic vessels was mainly done by the so-called “hot spot” analysis³⁰ which usually considers only small tissue regions where density of lymphatic vessels was the highest. In contrast, our approach consisted of automated marker quantification in large but distinct tissue areas based on staining intensity. In order to validate the automated marker quantification method and characterize the best marker to identify LECs in the individual tissues, we performed automated quantification of Prox-1 and podoplanin, respectively, and correlated the results with our data from LEC counting by eye (see “LEC quantification” in Methods). We found that podoplanin quantified by automated whole tissue analysis correlated well with lymphatic vessels quantified per mm² by counting by eye in the different regions of the primary tumor (Fig. 1A) and in the tumor region of metastatic LNs (Fig. 1B). In agreement with our visual observation, automated quantification of Prox-1 did not correlate significantly with LEC counting by eye in primary tumor (Fig. 1A) and only minor in the tumor region of metastatic LNs (Fig. 1B) whereas the correlation for podoplanin was strong. In contrast to tumor bearing tissues, LEC quantification in tumor-free LNs was superior based on Prox-1 staining as compared to podoplanin staining, because podoplanin was also expressed by several other cell types in the lymph nodes, for example follicular dendritic cells (Fig. S1C). Indeed, automated quantification of Prox-1 showed a good correlation with the LEC counting by eye in tumor-free LNs (Fig. S1D). The combined use of both, Prox-1 and podoplanin by Immunofluorescence (IF) labeling confirmed the validity of our strategy to identify LECs in the different tissues analyzed (Fig. 1C). Therefore, based on these results, we chose for our broad quantification of LECs to use podoplanin expression in primary tumors and the tumor regions of metastatic LNs, and Prox-1 expression in tumor-free LNs.

Increased intratumoral lymph vessel density (LVD) and VEGF-C in earliest stages of primary melanoma

High LVD has been previously described in prominent “hot spots” both within and around primary cutaneous malignant melanoma.³¹ Moreover, melanoma lesions have been shown to have higher intratumoral and peritumoral LVD compared to benign melanocytic lesions, likely due to pro-lymphangiogenic factors, essentially VEGF-C, secreted by tumor cells.³²⁻³⁴ Detailed analysis of the distribution of LECs in primary tumors showed that LVD was already increased in the earliest stage of melanoma (melanoma *in situ*) in comparison to the adjacent normal skin. Furthermore our data confirmed that LVD is increased in primary melanoma, specifically in the invasive margin and the peritumoral regions (Fig. 2A). In order to

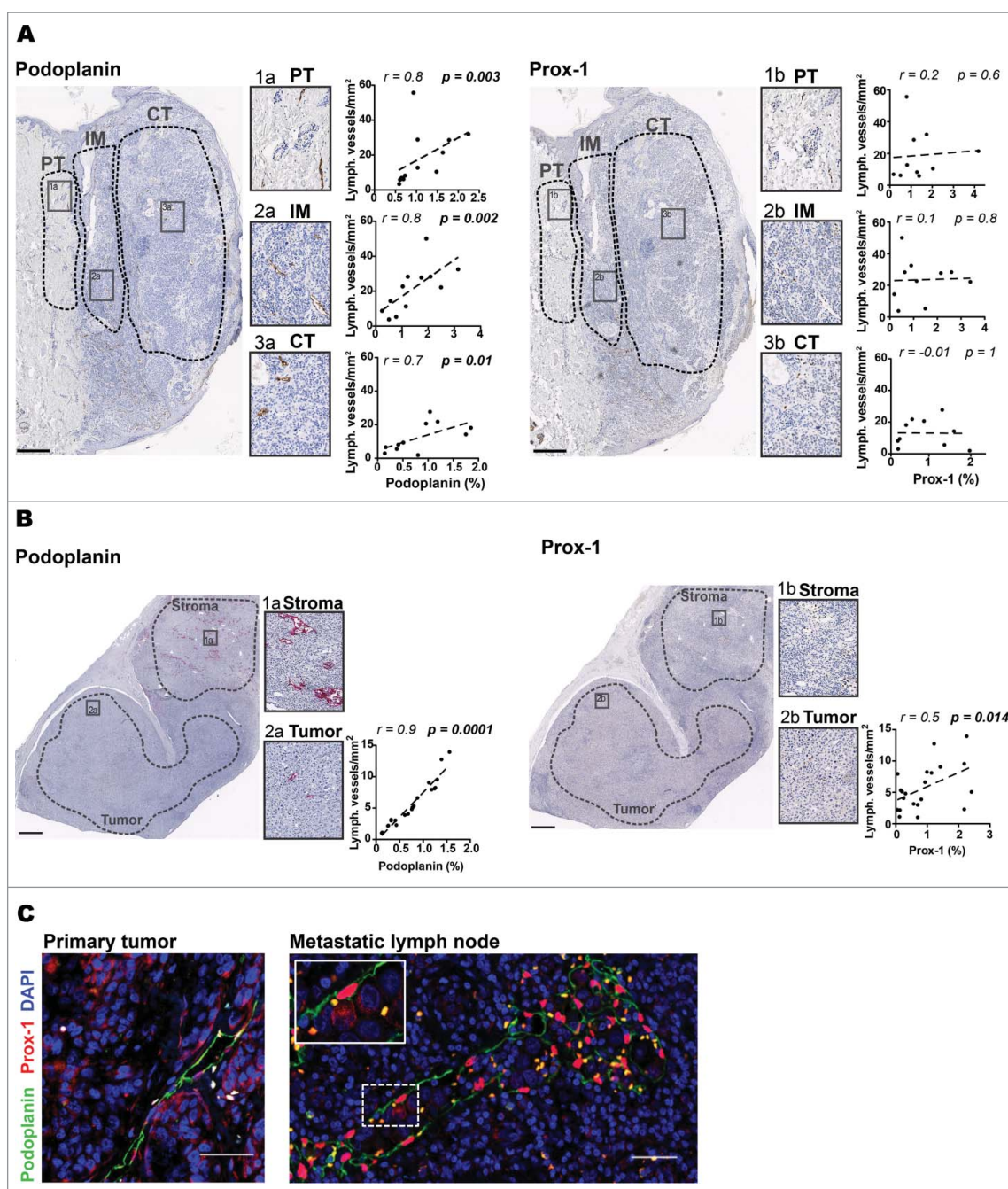


Figure 1. Comparison of lymph vessel density (LVD) assessment by automated pixel based large-scale quantification versus LEC counting by eye. Representative immunohistochemistry images showing podoplanin and Prox-1 staining of peritumoral area (PT), invasive margin (IM) and center of tumor (CT) of A) primary melanoma and B) stroma and tumor regions of metastatic lymph node sections (Scale bars in A) 500 μm ; in B) 1mm). Correlations of podoplanin or Prox-1 (% of pixel positive cells) counted by the ImageScope™ software (x-axis) versus counted by eye (y-axis) in IM (n = 12), CT (n = 11) and PT (n = 12) of primary tumors and in tumor regions of metastatic LNs (n = 22). C) Representative immunofluorescence images of podoplanin (green) and Prox-1 (red) co-localization in different tissues (20X, scale bar = 50 μm , DAPI, blue). All correlations were analyzed using non-parametric Spearman's test. (PT): peritumoral area, (IM): invasive margin, (CT): center of tumor.

determine the presence of VEGF-C and its association with LEC formation and distribution we performed immunostaining of VEGF-C in primary tumors and metastatic lymph nodes. Podoplanin positively correlated with VEGF-C only within melanoma *in situ* (Fig. 2B) while in primary melanoma and in the tumor regions of metastatic LNs these parameters did not correlate (Fig. S2A-F). These results are compatible with the notion that VEGF-C may play a role in lymphangiogenesis in early stage of melanoma formation.

LVD correlates with tumor infiltrating CD8⁺ T cells and expression of immune suppressive molecules

To investigate the potential associations of LVD with immune cell infiltrates, we next quantified the density of infiltrating lymphocytes expressing CD8, CD4, Foxp3 and CD19. Since LNs are important sites for tumor spread and immune responses, we not only analyzed the immune microenvironment of primary tumors, but also the one of the tumor regions within

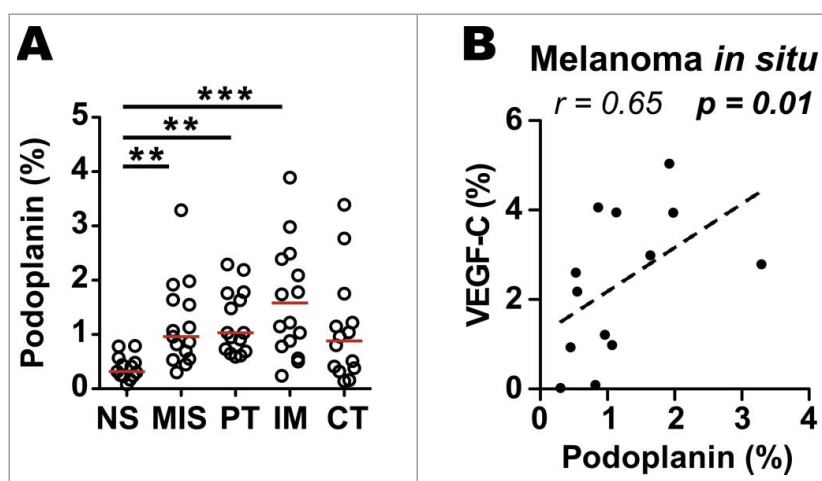


Figure 2. Increased lymphatic vessel density (LVD) in melanoma *in situ*, invasive margin and peritumoral area of primary melanomas. A) Quantification of podoplanin density (% of pixel positive cells) in normal skin (NS; $n = 12$), melanoma *in situ* (MIS; $n = 14$) and in the different histological zones of primary melanomas, i.e. peritumoral region (PT; $n = 13$), invasive margin (IM; $n = 13$) and center of tumor (CT; $n = 12$). Line indicates median. ***, $p \leq 0.001$; **, $p \leq 0.01$; one-way Kruskal-Wallis non-parametric test with post-hoc test Dunn correction. B) Correlation of podoplanin with VEGF-C density (% of pixel positive cells) in melanoma *in situ* ($n = 13$). Correlation was analyzed using non-parametric Spearman's test.

metastatic LNs. Interestingly, similar to the distribution of LECs we found the highest density of $CD8^+$ T cells in peritumoral areas and the invasive margin of primary tumors (Fig. 3A). Quantitative analysis revealed that primary tumors showed strong positive correlations of $CD8^+$ T cell infiltration with LVD (Fig. 3B). This correlation held true in all primary tumor regions analyzed (center of tumor, invasive margin and peritumoral regions). However, LVD showed only positive trends not reaching statistical significance for $CD4^+$ cells, $CD19^+$ cells and $FoxP3^+$ regulatory T cells within primary tumors (Fig. S3A-C). A strong positive correlation between LVD and $CD8^+$ T cells was also found in metastatic LNs (Fig. 3C). In contrast to primary tumors, in metastatic LNs we found positive associations between LVD and $CD19^+$ cells and also with $FoxP3^+$ cells (Fig. 3D), suggesting attraction of potentially immune suppressive cells by mechanisms involving lymphatic vessels. Together, these data propose that lymphangiogenic regions within the tumor may specifically chemoattract circulating T cells, consistent with studies in mouse melanoma, where VEGF-C was shown to upregulate CCL21 to attract $CCR7^+$ immune cells.²⁴

Next, we investigated the correlation of LVD with the presence of immune suppressive factors by analyzing the expression of iNOS, IDO, and arginase-1 (Arg-1) in the same tissues. IF analysis revealed that both iNOS and IDO were mainly produced by cells surrounding lymphatic vessels rather than by the LECs in primary tumors (Fig. 4A, left panels). However, we found iNOS expression in the cytoplasm of LECs in metastatic LNs (Fig. 4A, right panels) suggesting that tumor-associated LECs can play direct roles in immune modulation. LVD positively correlated with iNOS expression in the invasive margin, and with IDO expression in the center of tumor (Fig. 4B, left panels). In the tumor region of metastatic LNs, iNOS and IDO expression were positively correlated with LVD (Fig. 4B, right panels). Arg-1 was neither expressed by LECs nor associated with LVD in any of the melanoma tissues analyzed (Fig. S4A and B).

VEGF-C correlates with T cell infiltration in primary melanoma and immune suppressive molecules in early stages of primary melanoma and metastatic LNs

Mouse melanomas have been reported to pre-condition future sites of LN metastasis by enhancing lymphangiogenesis, inducing an immune tolerant microenvironment and thus impairing the development of anti-tumor immunity.^{35,36} Furthermore, VEGF-C overexpression in mouse melanoma promoted an immune suppressive microenvironment in primary and downstream LNs.^{24,25} To address the potential role of VEGF-C in modulating host anti-tumor immunity in human melanoma, we quantified tumor sections immunostained for VEGF-C and immune markers. Interestingly, in the earliest stages of primary melanoma (melanoma *in situ*), we found strong positive correlations between VEGF-C expression and iNOS (Fig. 5A). Increased expression of VEGF-C correlated with elevated expression of iNOS and IDO in tumor regions of metastatic LNs (Fig. 5B-C). These results suggest that VEGF-C may have different roles in modulating the tumor microenvironment (TME) depending on tumor stage and tissue location.

LVD correlates with $CD8^+$ T cells and immune suppressive molecules in tumor-free LNs adjacent to metastatic LNs

Mouse studies have suggested that melanomas can secrete factors that pre-condition potential future metastatic sites in LNs, and that this pre-conditioning is associated with increased LVD.^{35,36} Studies in humans have shown immunological differences in LNs close to the primary melanoma as compared to the more remote LNs, with regard to the capacity of paracortical dendritic cells and T cells to inhibit or enhance melanoma cell growth *in vitro*, as well as the density of high endothelial venules (HEVs).³⁷ To identify possible changes in distal LNs in our patients, we analyzed 23 tumor-free LNs, with the hypothesis that tumor-free LNs may differ depending on whether they were from LN dissections with one or more metastatic LNs

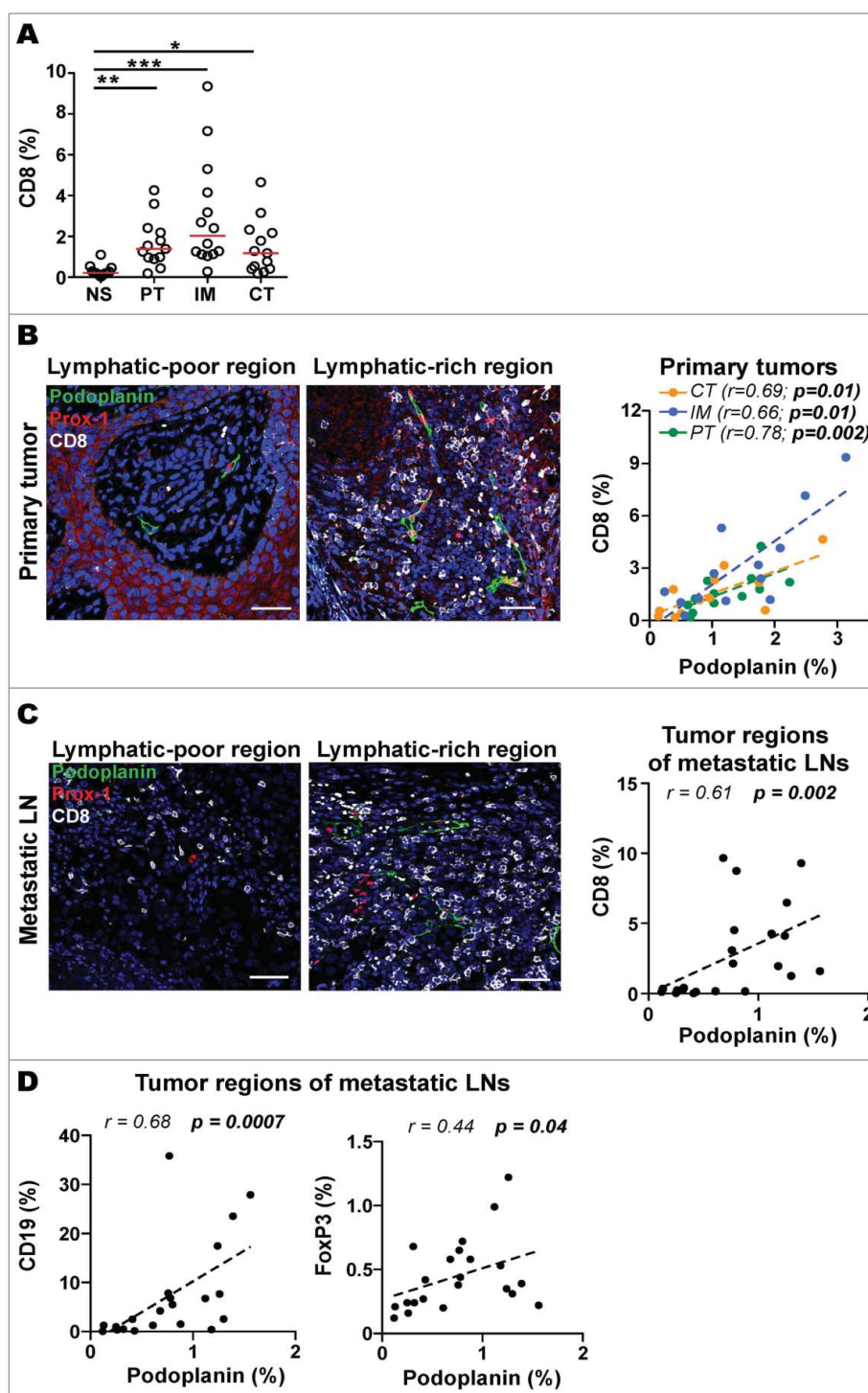


Figure 3. LVD correlates with infiltration of CD8⁺ T cells in primary tumors and tumor regions of metastatic lymph nodes (LNs). A) Quantification of CD8 density (% of pixel positive cells) in different zones of primary melanomas. Statistical significance was calculated using one-way Kruskal-Wallis non-parametric test with post-hoc test Dunn correction. Line indicates median. ***, $p \leq 0.001$; **, $p \leq 0.01$; *, $p \leq 0.05$. Representative immunofluorescence images showing lymphatic vessels (Prox-1, red; podoplanin, green) and CD8⁺ T cells (grey) in lymphatic-poor and -rich regions of B) primary tumor and C) metastatic LN (20X, Scale bar = 50 μ m, DAPI, blue). Correlations of podoplanin with CD8 density (% of pixel positive cells) in PT (n = 13), IM (n = 13) and CT (n = 13) of B) primary tumors and in C) metastatic LNs (n = 23). D) Correlations of podoplanin with CD19 (n = 21) and FoxP3 (n = 22) density (% of pixel positive cells) in tumor regions of metastatic LNs. All correlations were analyzed using non-parametric Spearman's test. (PT): peritumoral region, (IM): invasive margin, (CT): center of tumor.

(tumor-positive LN dissection; n = 14) versus dissections where all LNs were tumor-free (tumor-negative LN dissection; n = 9). Interestingly, tumor-free LNs from positive LN dissections had higher expression of Prox-1 as compared to LNs from negative LN dissections (Fig. 6A). Greater densities of CD8⁺ cells and CD4⁺ cells were seen in LNs from tumor-

positive LN dissections compared to negative LN dissections (Fig. 6B). In line with this, higher density for iNOS and Arg-1 were found in LNs from positive LN dissections (Fig. 6C). Interestingly, in tumor-free LNs from positive LN dissections, LECs were found to express iNOS (Fig. 6D), showing a positive correlation with iNOS expression (Fig. 6E) similar to that in

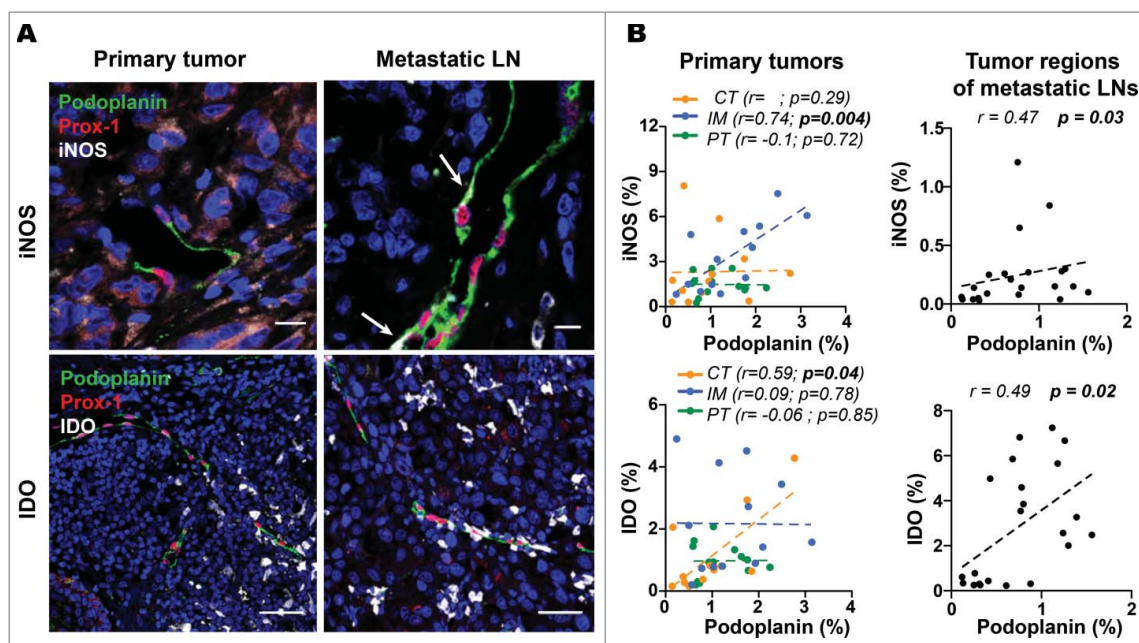


Figure 4. LVD correlates with expression of immune suppressive molecules in primary tumors and tumor regions of metastatic LNs. A) Representative immunofluorescence images in a section of a primary tumor and a metastatic LN showing that intratumoral lymphatic vessels (Prox-1, red; podoplanin, green) express iNOS (white, arrows) in metastatic LNs and do not express IDO (grey) in either location (63X upper panels Scale bar = 10 μ m, and 40X lower panels, Scale bar = 50 μ m, DAPI, blue). B) Correlations of podoplanin with iNOS and IDO density (% of pixel positive cells) in IM (n = 13), CT (n = 12) and PT (n = 13) of primary tumors and in metastatic LNs (n = 23). Correlations were analyzed using non-parametric Spearman's test. (IM): invasive margin, (CT): center of tumor, (PT): peritumoral region.

metastatic LNs (Fig. 4B). Together, these data indicate that tumor-free LNs adjacent to metastatic LNs have increased LVD, lymphocyte density and immunosuppressive features compared to LNs from tumor negative LN dissections.

Discussion

Multiple studies have demonstrated the clinical relevance of tumor-associated lymphatics and their involvement in malignant spread.³⁸⁻⁴⁰ In human melanoma, increased intra- and peritumoral LVD as well as the lymphatic growth

factor VEGF-C strongly correlate with metastatic dissemination.^{17,33,41-43} Lymphatic vessels may support migration of tumor cells, but may also modulate immune cells, as recently demonstrated in primary tumors and draining LNs in mice,^{24,25,44} raising the possibility that lymphatics mediate immune suppression and poor clinical outcome in cancer patients.^{19,31,42} Because corresponding human data are missing, we performed a very wide IHC analysis. Our findings reveal multiple correlations between lymphatic vessels and host immunity, suggesting immune mechanisms that act locally as well as loco-regionally in melanoma patients (Fig. 7).

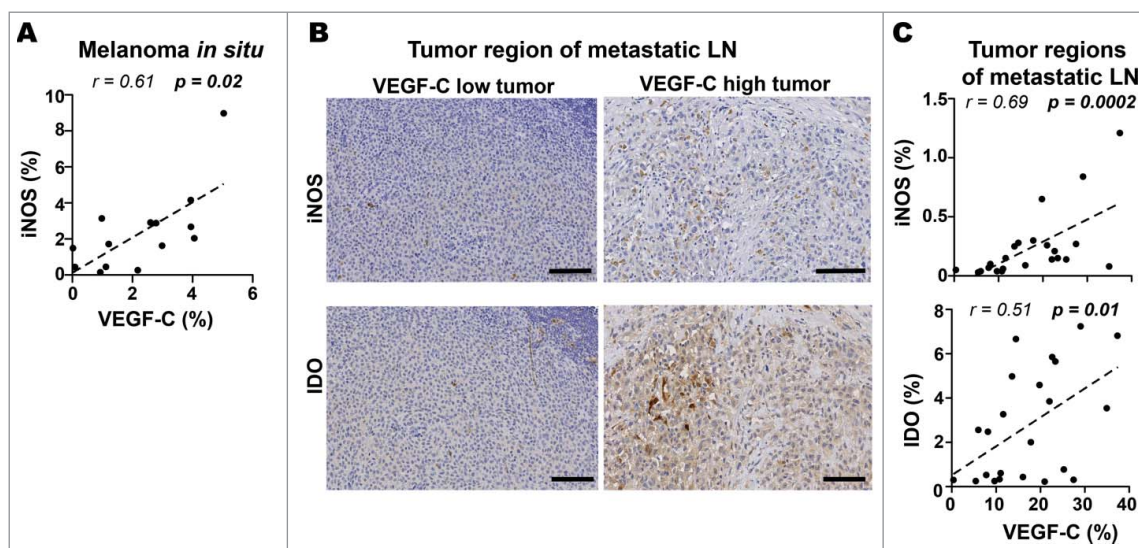


Figure 5. VEGF-C is associated with expression of immune suppressive molecules in melanoma *in situ* and tumor regions of metastatic LNs. A) Correlations of VEGF-C with iNOS density (% of pixel positive cells) in melanoma *in situ* (n = 14). B) Representative immunohistochemistry images showing iNOS and IDO expression in tumor region of VEGF-C-low and VEGF-C-high metastatic LN sections (Scale bar = 100 μ m). C) Correlations of VEGF-C with iNOS (n = 23) and IDO (n = 23) density (% of pixel positive cells) in tumor regions of metastatic LNs. Correlations were analyzed using non-parametric Spearman's test. (IM): invasive margin, (CT): center of tumor, (PT): peritumoral region.

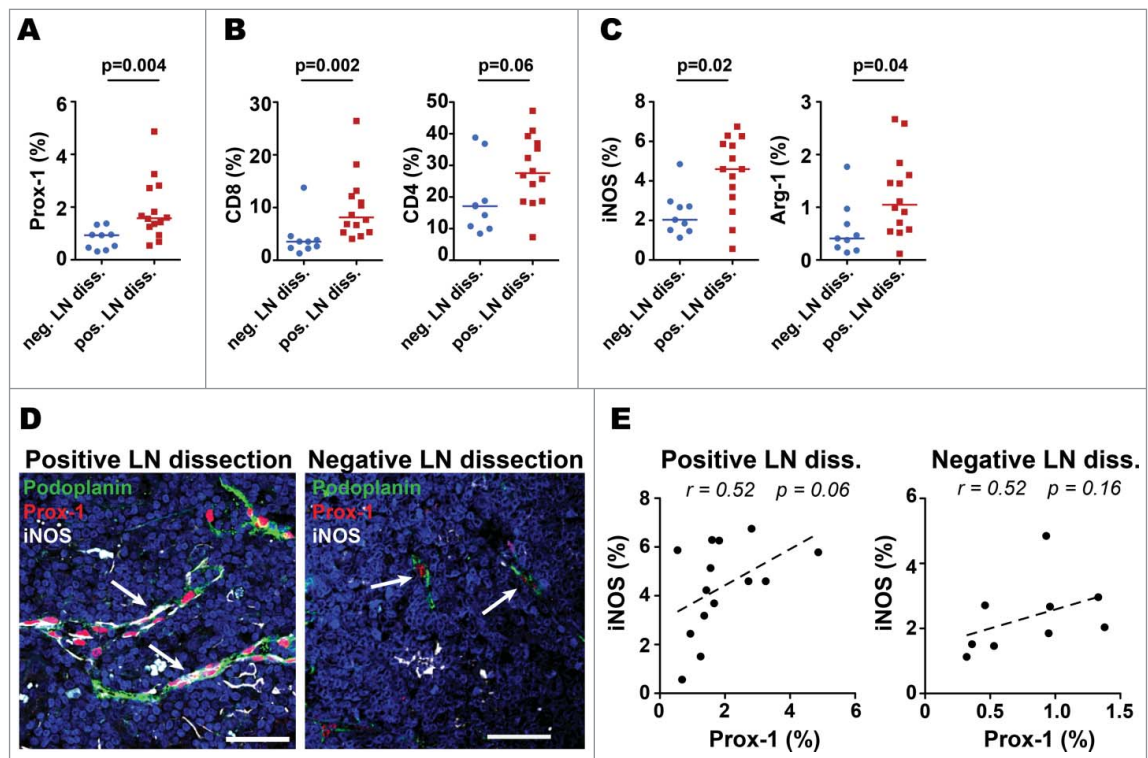


Figure 6. Tumor-free LNs that are adjacent to metastatic LNs have higher LVD, T cell infiltration and immune suppressive molecules than LNs from completely tumor-free LN-regions. Tumor-free LNs from negative LN dissections (neg. LN diss.; $n = 9$) were compared with tumor-free LNs from positive LN dissections (pos. LN diss.; $n = 14$). Density of A) lymphatic vessels, B) T cells and C) the immune suppressive molecules iNOS and Arg-1 (% of pixel positive cells). Line indicate median; data were analyzed with the unpaired t-test for normally distributed data sets and with a nonparametric unpaired Mann-Whitney U test for data sets that were not normally distributed. D) Representative immunofluorescence images showing that intratumoral lymphatic vessels (Prox-1, red and podoplanin, green) mainly expressed iNOS (white, arrow) in tumor-free LNs from positive LN dissections. Scale bars = $50\mu\text{m}$, Arrow bar highlighting lymphatic vessel structures. E) Correlations of Prox-1 with iNOS in tumor-free LNs from negative and positive LN dissections (% of pixel positive cells). Correlations were analyzed using non-parametric Spearman's test.

A standard methodology of lymphatic vessel quantification is based on the observation that lymphatics form areas of increased LVD density.⁴⁵ The majority of studies on LVD and clinical outcome of melanoma patients have used staining quantification methods based on visual inspection and selection

of "hot spots" (e.g. Weidner and Chalkley method).^{32,46,47} Despite the recent emergence of computer-assisted image analysis that reduces the variability and subjectivity in quantifying lymphatics, many studies are still based on either selected "hot spot" regions or randomly selected fields.^{16,43} We analyzed

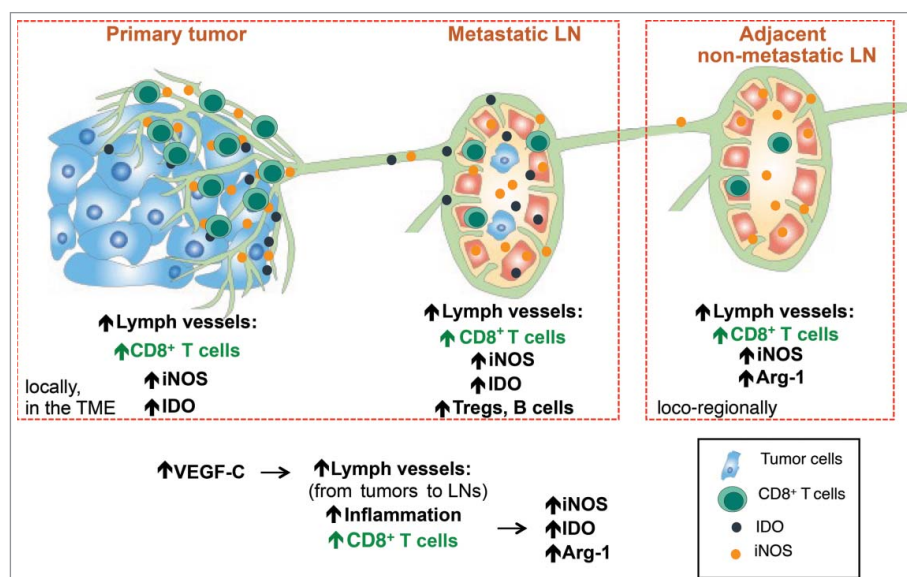


Figure 7. Increased lymphatic vessels density is associated with increased CD8⁺ T cell infiltration, together with increased expression of immunosuppressive molecules such as iNOS, IDO and Arg-1. This can be observed not only locally in primary tumors and metastatic lymph nodes (LNs) but also in adjacent non-metastatic LNs. Together, tumor derived VEGF-C induces lymphatic vessels that attract CD8⁺ T cells, with their known fundamental properties, namely the promotion of anti-tumor immune responses but also immune suppression (via adaptive immune resistance mechanisms).

specific regions as well as entire sections of different melanoma-associated tissues with a dedicated image analysis software, allowing quantitative assessment of unusually large tissue areas in a reproducible manner. Specifically, we used the pixel count algorithm (ImageScopeTM, Aperio) for large-scale quantification of lymphatics, lymphocytes and immune suppressive molecules. Pixel-based analysis has been validated as an accurate strategy for the assessment of cell density in tissue sections,⁴⁸ and may be more precise than cell-counting algorithms, especially in the setting of dense and relatively homogenous cell populations such as within the tumor mass.

In agreement with our findings, increased LVD has been described in and around primary melanomas compared to melanocytic nevi and normal dermis.³²⁻³⁴ We did not find statistically significant differences between intra- (either center of tumor or invasive margin) or peri-tumoral LVD as described by some^{46,49,50} but not other studies.^{43,51} Possible reasons for discrepancies could be the use of different image analysis and/or staining quantification strategies.

Many reports established the role of VEGF-C in promoting lymphangiogenesis and LN metastases in murine and human tumors.⁵² Nonetheless, VEGF-C expression did not always correlate with LVD in cutaneous melanoma.⁴⁶ Surprisingly, we found that VEGF-C correlated with LVD only in the earliest stage of primary melanoma. This suggests that VEGF-C mainly promotes lymphangiogenesis early in the development of the tumor.

Recently it was shown that tumor-associated lymphangiogenesis mediated intratumoral T cell infiltration in mice.²⁹ Our findings indicate that similar mechanisms are in place in humans, because LVD strongly correlated with CD8⁺ T cell infiltration in primary cutaneous melanoma as well as in metastases of draining LNs. Interestingly, these associations were found in the three different zones delimited in the primary tumor sections, implying that lymphatic activation may promote accumulation of CD8⁺ T cells not only around but also within the tumor mass.

Besides LECs, tertiary lymphoid structures (TLSs) are important components of tumor-associated immune functions. TLS are of increasing interest in tumor immunology because they are often associated with anti-tumor T cell responses and favorable prognosis of cancer patients.⁵³ Although high endothelial venules (HEVs) have been described in primary melanoma and have been linked to good clinical outcome,^{54,55} conflicting results exist in regard to the presence of TLSs in primary melanoma, in spite of the fact that the latter frequently contain HEVs.^{56,57} While we found a positive association between lymphatics and CD19⁺ cells in metastatic LNs, we did not detect many B cell clusters in the tumor samples examined here. The increased infiltration of B cells in association with lymphatic vessels in metastatic LNs may support the notion that lymphatics promote also the humoral immune response. Further investigations are required to elucidate the interactions between lymphatics and B cells, and their roles in cancer patients.

LECs can affect T cell fate as well as suppress dendritic cell-mediated T cell activation by secreting a variety of immune suppressive factors such as TGF- β , IDO and iNOS.⁵⁸ Kornek et al. reported that *in vitro*-expanded murine LECs mediated direct suppression of T cell proliferation, essentially depending on IFN- γ from activated T cells.⁵⁹ Nörder et al. demonstrated that human *in vitro* IFN- γ activated LECs produced IDO which

suppressed T cell activation.⁶⁰ Compatible with these *in vitro* studies, we observed significant associations between LVD and iNOS expression at the invasive margin and IDO expression in the center of tumor of primary melanomas, but also found significant correlations with CD8⁺ T cell infiltration.

In concert with primary tumors, our study identifies immune suppressive molecules in tumor-draining LNs, suggesting that immune mechanisms operating in metastatic LNs^{25,37,61,62} may at least in part be similar to those in primary tumors.⁶³ In contrast to primary tumors, we found a significant correlation between LECs and FoxP3⁺ lymphocytes. The question of whether regulatory T cells play an important role in melanoma progression and metastasis formation is still unanswered, and conflicting data have been reported with regard to clinical impact.⁶⁴

Several studies have identified alterations in both local and regional immune functions of metastatic LNs that may contribute to tumor expansion and metastasis formation.³⁷ However, only limited data exist showing possible effects of nearby metastases on immune functions of tumor-free LNs. Zuckerman et al. examined differences in immune cell signatures between tumor-free LNs of node negative breast cancer patients and tumor-invaded sentinel lymph nodes (SLNs), tumor-free SLNs or tumor-free non-sentinel lymph nodes (NSLNs) of node positive breast cancer patients.⁶⁵ This study provided the first evidence of altered immune regulation depending on whether neighboring LNs were metastatic or not. We investigated the immunological differences between tumor-free LNs from patients with positive versus negative LN dissections. Our data show that the tumor-free LNs from tumor-positive LN dissections had higher densities of LECs, T lymphocytes, iNOS and Arg-1, as compared to those from negative LN dissections, arguing that lymphatics may impact on immune regulation beyond the TME and prior to metastasis formation.

Together, we describe novel associations between LECs, lymphocytes and immune suppressive molecules within different tissues of melanoma patients. LECs were positively associated with locally enhanced CD8⁺ T cell infiltration as well as iNOS and IDO expression within primary melanoma tissues and in metastatic LNs. Tumor-free LNs showed similar associations, pointing to loco-regional effects. These results support the view that LECs are active modulators of anti-tumor immune responses within different human melanoma tissues. Our results should be validated in larger numbers of patients. Furthermore, as our study could only reveal correlations, further studies will be needed to refine the underlying mechanisms, e.g. by *ex-vivo* functional analysis combined with systems biology approaches and mechanistic mouse studies.

A major aim in the development of cancer immunotherapies is to overcome suppression of anti-tumor T cell responses. Our study suggests that LECs are implicated in the recruitment and attraction of CD8⁺ T cells as well as the expression of immune suppressive molecules. Therefore, LECs likely support both, promote and hinder anti-tumor T cell responses. Of note, the presence of a T cell-inflamed tumor microenvironment is indicative of an endogenous adaptive immune response against a given tumor, and is emerging as a useful predictive biomarker for response to immunotherapy.⁶⁶ Indeed, it was recently shown that highly infiltrated and lymphangiogenic murine tumors were more sensitive to immunotherapy, by recruiting T cells and antigen presenting cells through the

CCL21-CCR7 axis. Furthermore, serum VEGF-C was found to correlate with antitumor T cell responses and progression free survival of melanoma patients treated with immunotherapy.⁶⁷ Finally, therapeutic induction of lymphoid structures synergized with immunotherapy in mice.⁶⁸ Thus, novel combination immunotherapies may include the promotion of lymphatics despite that they are also implied in immune suppressive mechanisms and metastatic spread. Future therapy improvements may depend on the successful increase of the beneficial roles of lymphatics with simultaneous reduction of their negative effects.

Patients and methods

Patients

This study investigated 29 metastatic melanoma patients that had been included in a phase I vaccination trial (LUD 00-018 study, ClinicalTrials.gov Identifier NCT00112229) at the Ludwig Cancer Research Center (LICR, University Hospital, Lausanne, Switzerland) between 2003 and 2011 (Table S1), as described previously.^{69,70} Briefly, 29 HLA-A2⁺ patients with histologically proven metastatic melanoma of the skin expressing Melan-A/MART-1 received 1–4 cycles of monthly subcutaneous vaccinations with 100 μ g Melan-A/MART-1 A27L analog or native peptide (\pm a Tyrosinase peptide) and CpG-7909 (500 μ g PF-3512676/7909; provided by Pfizer/Coley Pharmaceutical Group) emulsified in incomplete Freund's adjuvant (300–600 μ l Montanide ISA-51; provided by Seppic). The patients were evaluated for treatment toxicity, immune response (CD8⁺ T cell response), tumor response and survival (Table S2). Of the 29 patients included in the study, 25 were selected for the present analysis and 4 were excluded (one patient had uveal melanoma and three patients did not have any FFPE tissues available). 19 primary melanoma samples from 15 patients, 33 metastatic LNs from 14 patients (23 metastatic LNs were taken before the vaccination and 10 metastatic LNs were taken long after the end of the vaccination trial) and 23 tumor-free LNs from 20 patients (17 tumor-free LNs were taken before the vaccination and 6 tumor-free LNs were taken long after the end of the vaccination trial) were obtained and were analyzed for their lymphocyte populations, lymphatic vessels and immunosuppressive molecules. 14 tumor-free LNs from 12 patients were from tumor-positive LN dissection and 9 tumor-free LNs from 8 patients were from tumor-negative LN dissection. The study was approved by the Ethics Committee of Canton of Vaud and the regulatory authorities, and conducted in compliance with all legal and regulatory requirements.

Immunohistochemistry (IHC)

Chromogenic IHC staining

4- μ m tick tissue sections of patient's formalin-fixed paraffin-embedded (FFPE) tissue specimen's were first deparaffinised in xylene and rehydrated by sequential incubation in EtOH/water solutions. Tissues were then treated with 3% H₂O₂ in distilled water for 5 minutes to quench endogenous peroxidase activity. Heat-induced antigen retrieval was performed in Tris-EDTA buffer (pH 9) for 1'30" in a steamer. Subsequently, sections were incubated at room temperature

with primary antibodies to CD8 (clone C8/144b, Dako, 1:30, 32 min), CD4 (clone 4B12, Novocastra, 1:10, 90 minutes), CD19 (clone BT51E, Novocastra, 1:50, 32 min), FoxP3 (clone 236a/E7, Abcam, 1:50, 60 min), podoplanin (clone D2-40, Covance, 1/400, 60 min), Prox-1 (R&D, 1:100, 32 min), VEGF-C (Invitrogen, 1:20, 40 min), IDO (from Brussels, 1:500, 40 min), iNOS (Thermoscientific, 1:75, 40 min), Arg-1 (Mybiosource, 1:300, 40 min), Melan-A (clone A103, Dako, 1:50, 32 min), melanosome (clone HMB45, Dako, 1:50, 32 min) and S100 (Novocastra, 1:800, 40 min) followed by a secondary anti-mouse (K4001, Dako), anti-rabbit (DK4003, Dako) or anti-goat antibody (Histofine RTU-Biosciences) RTU/HRP ENVISION for 30 minutes. 3-amino-9 ethylcarbazole (AEC) was used as a red chromogen (K3464, Dako) for CD4, S100, Melan-A and melanosome and Diaminobenzidine (DAB, K3468, Dako) as a brown chromogen (K3468, Dako) for the rest of the antibodies. After rinsing with water, sections were counterstained with Hematoxylin Gill II (Merck 1.05175) and coverslipped with xylol. CD8, CD4, CD19, FoxP3, podoplanin, Prox-1, Melan-A, S100 and Melanosome were done on Ventana BenchMark machine using Cell Conditioning 1 (CC1, 950-124, Ventana) as a buffer for heat-induced antigen retrieval with varied time for the different antibodies, other reagent and time was done as described above. iNOS, VEGF-C, Arg-1 and IDO stainings were done manually by the technician with the above-mentioned protocol. Positive controls included tonsil, lung, liver and colon. Immunostainings with appropriate isotype control antibodies were used as negative controls. For illustration purpose, representative images of the different stainings were taken from tumor-free LNs (Fig. S5).

Conventional immunofluorescence (IF) staining

As for chromogenic IHC staining, 4- μ m tick tissue sections were first deparaffinised in xylene and rehydrated by sequential incubation in EtOH/water solutions. Antigen retrieval was performed by 15 minute incubation in boiling Tris-EDTA buffer (pH 9), following 30 minutes incubation in blocking solution (TBS+0.01% Triton X-100+2%BSA+2%total serum from host secondary antibody). Sections were incubated overnight at 4°C with primary antibodies to CD8 (clone C8/144b, Dako, 1:30), podoplanin (clone D2-40, Covance, 1/200), Prox-1 (R&D, 1:100), iNOS (Thermoscientific, 1:75), Arg-1 (Mybiosource, 1:300), IDO (from Brussels, 1:500), CCL21 (Atlas antibodies, 1:200) and PD-L1 (Cell Signaling, 1:200). Alexa Fluor 488-labeled donkey anti-mouse IgG (Invitrogen, 1:400), 568-labeled donkey anti-goat IgG (Invitrogen, 1:600) and 647-labeled donkey anti-rabbit IgG (Invitrogen, 1:800) antibodies were used as secondary antibodies and incubated for 1 hour at room temperature. After stringent washes, sections were counterstained with DAPI (Vector Laboratories, Burlingame, CA) for 5 minutes and coverslipped with mounting medium (Vectashield mounting media). Positive controls were done on tonsils, LNs and skin tissues. Negative slides used TBS instead of primary antibody, with other conditions constant. Images were obtained with confocal microscope ZEISS LSM 700 UPRIGHT.

Image analysis

In primary melanoma, four relevant histological regions were defined: invasive margin (IM, defined as a tumor region of about 400- μm width between the tumor and the reticular dermis), center of tumor (CT), peritumoral region (PT, defined as a region of about 400- μm width in the dermis surrounding the invasive margin), and normal skin (NS, determined as a region of about 200- μm width separated by at least 1mm from tumor cells), as illustrated in Fig. S6A. IM, CT and PT were present in 13 sections of the 19 primary melanoma selected and analyzed (Table S3). The other 6 primary melanoma samples, the tumor mass were too small or confined in the epidermis such that these three zones could not be defined. Normal skin was identified in 12 primary tumor samples. We also selected 14 sections from 10 melanoma patients where tumor cells were still confined in the epidermis and have not grown deeper. Those are referred to as melanoma *in situ* (Table S3). Tumor cells were identified based on Melan-A, Melanosome (HMB45) and S100 positive staining or morphological criteria (large atypical and pleomorphic cells with abundant eosinophilic cytoplasm, visible nucleoli and mitosis) when all three markers were negative.

For the analysis of LN metastases, we pre-selected 33 metastatic LNs from 14 melanoma patients. 10 metastatic LNs were excluded from the analysis because of the presence of large regions of tumor necrosis (2/10), presence of excessive melanin pigments rendering analysis impossible (5/10), tumor metastasis size less than 1 mm² (1/10) or tumor metastasis size more than 98% of the entire LN (2/10). In the 23 remaining metastatic LNs, we defined 2 different zones corresponding to center of tumor and stroma (Fig. S6B). The center of tumor was determined as previously described for primary tumors. Stroma was defined as connective tissue surrounding the tumor cells (present in 14 (61%) metastatic LNs). Finally, we also studied tumor-free LNs that had been obtained through LN dissection surgery. We analyzed the total area without defining specific zones in these 23 tumor-free LNs (Table S4). Image analyses and determination of regions were approved by two blinded experienced pathologists.

Staining quantification

ImageScope™ Aperio software

Whole slide digital images were obtained for each specimen stained with Chromogenic IHC staining using NanoZoomer 2-HT digital slide scanner (Hamamatsu). The resulting high-resolution digital images were analyzed with the ImageScope™ software, version 12.1 (Aperio Technologies, Vista, CA, USA), using the pixel positive cell algorithm 9.1 as previously described and validated.⁴⁸ Briefly, this algorithm detects pixels that match input parameters set for the algorithm and generates four output values based on the pixel's color range: haematoxylin or negative signal (blue in mark-up image), weak positive (yellow in mark-up image), positive (orange in mark-up image) and strong positive

(brown in mark-up image) (Fig. S7). Using these parameters, the strong non-specific (brown) as well as the weak positive (yellow) signals were considered as debris background staining, whereas the positive value (orange) was considered as specific. Folds, debris, holes were also removed manually to be excluded from the staining quantification analysis. Quantification of the staining in the tissue selected was reported as a relative abundance ratio, which was based on the number of positive pixels (orange) divided by the total number of pixels (blue + yellow + orange + brown). The relative abundance ratio was reported in % and represented the percentage of density per tissue area for the quantified staining. Results obtained were controlled to match with visual inspection. The pixel positive cell algorithm was applied on primary tumors, tumor-free LNs and metastatic LNs.

Quantification of LECs

LECs are typically identified by expression of the nuclear transcription factor Prox-1 and the surface markers podoplanin and Lyve-1. However, depending on their tissue location and state of development, LEC expression of these markers can be variable, and furthermore, other cell types within the tumor microenvironment can also express these markers.^{45,71} Some tumor-associated macrophages express Lyve-1, and cancer-associated fibroblasts found in the stroma can express podoplanin. As expected, in our tissue sections, LECs expressed podoplanin and nuclear Prox-1 in all tissues analyzed, but these markers were also found in other types of cells depending on the region evaluated (see result section and Fig. S1). Consequently, when comparing expression in the same tissue sections, Prox-1 and podoplanin did not necessarily correlate in the tumor regions (i.e. center of tumor and invasive margin) (Fig. S8). Indeed, we noticed a positive trend in peritumoral area and a positive correlation in normal skin, underlining that the expression of Prox-1 was not a reliable marker of intratumoral LECs. For validation of our quantification strategy and the identification of lymphatic vessels, we counted the lymphatic vessels by eye in the different regions of primary tumors, in the tumor area of metastatic LNs and in the entire section of non-metastatic LNs by combining IHC markers (i.e. podoplanin or Prox-1) with vessel morphology. The counting by eye was done in the same regions as the automated image analysis, covering the whole areas. The number of lymphatic vessels per area was then divided by the total surface area, resulting in lymphatic vessels per mm² for each region.

Identification of LECs may be improved by simultaneously using multiple markers which can be achieved with multiplex IF techniques. However, good quality stainings and analysis of wide areas and whole tissue sections is difficult (staining must be homogenous) and was not possible at the time when this work was done. Therefore, we used single marker LEC identification using IHC, allowing large-scale assessment and quantification. In addition, we used IF images for illustration purpose and for in-depth analysis of correlations found in IHC.

Statistics

To compare only two data sets, unpaired t- tests (normal distribution of data points) or Mann–Whitney U tests (data points not normally distributed) were used to assess statistical significance. To visualize correlations of two different markers, raw data received from the pixel positive cell algorithm (ImageScope™, see Image Analysis) were plotted and a line with linear regression was fitted into the plot. Correlation coefficients were calculated using Spearman's non-parametric test. To compare multiple groups, One-Way Kruskal-Wallis non-parametric tests were applied with post-hoc test Dunn correction. A two-tailed *p* value of ≤ 0.05 was considered to be significant. Analyses were performed with Prism (version 6.0b, GraphPad Software, La Jolla, CA, USA). Statistics were approved by a certified statistician.

Grant support

This research was supported by the ISREC Foundation (Switzerland), the Cancer Research Institute (USA), Ludwig Cancer Research (USA), the Swiss Cancer League (3507-08-2014 and 3312-08-2013), the Swiss National Science Foundation (CRSII3_160708 and 320030-152856), SwissTransMed (KIP 18) and the Rector's Conference of the Swiss Universities (crusch), Alfred and Annemarie von Sick, the Wilhelm Sander Foundation, the European Research Council (AdG-323053), the Gabriela and Theodor Kummer Foundation (Switzerland), the Erna Hamburger Foundation (Switzerland) and the Société Académique Vaudoise (Switzerland).

Disclosure of potential conflicts of interest

No potential conflicts of interest were disclosed.

Acknowledgments

We are obliged to the patients for their dedicated collaboration. The authors gratefully acknowledge Susana Leubat, Véronique Noguét, Solange Gros and Isabelle Surchet for tissue processing and staining, Pascale Anderle for statistical advice, Alain Michel for slide scanning and the Pathology Departments of the Universities of Geneva, Neuchâtel, Sion, and Basel as well as Meditest, Promed and Synlabs for providing tissues. We also thank Bianca Martins-Moura, Angela Orcurto, Christine Geldhof, Paula Marcos Mondéjar, Loredana Leyvraz, Lana Kandalaf, Kim Ellefsen, Lionel Trueb, Pierre Combe, Sylvie Rusakiewicz, Amanda Lund, Daniel Hohl, Olivier Gaide, Laurence Feldmeyer, Krisztian Homicsko, Doug Hanahan and George Coukos for collaboration, support and expert advice, and thank Benoit Van den Eynde and Luc Pilotte for providing the IDO antibody.

Authors' contributions

Conception and design: N.B., M.A.B., M.M., M.A.S., D.E.S.

Development of methodology: N.B., M.A.B., P.O.G., M.A.S., D.E.S.

Acquisition of data: N.B., M.A.B., K.D.J., E.D., P.B., L.C., S.A.M., H.M.E.H., E.R.


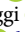

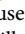
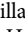
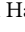




Analysis and interpretation of data: N.B., M.A.B., K.D.J., K.S., P.O.G., E.D., P.G.F., P.B., L.C., S.A.M., H.M.E.H., E.R., M.A.S., D.E.S.

Writing, review and revision of manuscript: N.B., M.A.B., K.S., P.O.G., M.F., N.W., T.M., K.I., M.M., M.A.S., D.E.S.

Technical and material support: I.L., P.Y., E.D., P.G.F., P.B., O.M., E.R.

Study supervision: M.A.S., D.E.S.

ORCID

Natacha Bordry  <http://orcid.org/0000-0002-3523-438X>
 Maria A. S. Broggi  <http://orcid.org/0000-0001-7909-5097>
 Kaat de Jonge  <http://orcid.org/0000-0003-2306-5555>
 Manuel Fankhauser  <http://orcid.org/0000-0001-7714-6524>
 Samia Abed-Maillard  <http://orcid.org/0000-0003-4773-8072>
 H el ene Maby-El Hajjami  <http://orcid.org/0000-0002-5786-5991>
 Kalliopi Ioannidou  <http://orcid.org/0000-0001-9097-4199>
 Igor Letovanec  <http://orcid.org/0000-0002-0410-3491>
 Maurice Matter  <http://orcid.org/0000-0003-1816-3003>
 Daniel E. Speiser  <http://orcid.org/0000-0003-2031-3250>

References

- Farkona S, Diamandis EP, Blasutig IM. Cancer immunotherapy: the beginning of the end of cancer? *BMC Med.* 2016;14:73. doi:10.1186/s12916-016-0623-5. PMID:27151159.
- Sharma P, Allison JP. Immune checkpoint targeting in cancer therapy: toward combination strategies with curative potential. *Cell.* 2015;161:205–14. doi:10.1016/j.cell.2015.03.030. PMID:25860605.
- Maus MV, Fraietta JA, Levine BL, Kalos M, Zhao Y, June CH. Adoptive immunotherapy for cancer or viruses. *Annu Rev Immunol.* 2014;32:189–225. doi:10.1146/annurev-immunol-032713-120136. PMID:24423116.
- Peggs KS, Quezada SA, Allison JP. Cancer immunotherapy: Costimulatory agonists and co-inhibitory antagonists. *Clin Exp Immunol.* 2009;157:9–19. doi:10.1111/j.1365-2249.2009.03912.x. PMID:19659765.
- Hamid O, Robert C, Daud A, Hodi FS, Hwu W-J, Kefford R, Wolchok JD, Hersey P, Joseph RW, Weber JS, et al. Safety and Tumor Responses with Lambrolizumab (Anti-PD-1) in Melanoma. *N Engl J Med.* 2013;369:134–44. doi:10.1056/NEJMoa1305133. PMID:23724846.
- Inoue H, Park J-H, Kiyotani K, Zewde M, Miyashita A, Jinnin M, Kuniwa Y, Okuyama R, Tanaka R, Fujisawa Y, et al. Intratumoral expression levels of PD-L1, GZMA, and HLA-A along with oligoclonal T cell expansion associate with response to nivolumab in metastatic melanoma. *oncoimmunology.* 2016;5:1–7. doi:10.1080/2162402X.2016.1204507.
- Ulloa-Montoya F, Louahed J, Dizier B, Gruselle O, Spiessens B, Lehmann FF, Suci S, Kruit WHJ, Eggermont AMM, Vansteenkiste J, et al. Predictive Gene Signature in MAGE-A3 Antigen-Specific Cancer Immunotherapy. *J Clin Oncol.* 2013;31:2388–95. doi:10.1200/JCO.2012.44.3762. PMID:23715562.
- Spranger S, Spaepen RM, Zha Y, Williams J, Meng Y, Ha TT, Gajewski TF. Up-Regulation of PD-L1, IDO, and Tregs in the Melanoma Tumor Microenvironment Is Driven by CD8+ T Cells. *Sci Transl Med.* 2013;5:200ra116–6. doi:10.1126/scitranslmed.3006504. PMID:23986400.
- Liu C, Peng W, Xu C, Lou Y, Zhang M, Wargo JA, Chen J, Li HS, Watowich S, Yang Y, et al. BRAF Inhibition Increases Tumor Infiltration by T cells and Enhances the Anti-tumor Activity of Adoptive Immunotherapy in Mice. *Clin Cancer Res.* 2013 Jan 15;19(2):393–403. doi:10.1158/1078-0432.CCR-12-1626.
- Taube JM, Anders RA, Young GD, Xu H, Sharma R, McMiller TL, Chen S, Klein AP, Pardoll DM, Topalian SL, et al. Colocalization of Inflammatory Response with B7-H1 Expression in Human Melanocytic Lesions Supports an Adaptive Resistance Mechanism of Immune Escape. *Sci Transl Med.* 2012;4:127ra37–7. doi:10.1126/scitranslmed.3003689. PMID:22461641.
- Ribas A. Adaptive Immune Resistance: How Cancer Protects from Immune Attack. *Cancer Discov.* 2015;5:915–9. doi:10.1158/2159-8290.CD-15-0563. PMID:26272491.
- Spranger S, Gajewski TF. Impact of oncogenic pathways on evasion of antitumor immune responses. *Nat Rev Cancer.* 2018;1–9. PMID:29217839.
- Netzer R, Fleishman SJ. Inspired by nature. *Science* 2016;352:657–8. doi:10.1126/science.aaf7599. PMID:27151851.
- Skobe M, Hawighorst T, Jackson DG, Prevo R, Janes L, Velasco P, Ricciardi L, Alitalo K, Claffey K, Detmar M. Induction of tumor

- lymphangiogenesis by VEGF-C promotes breast cancer metastasis. *Nat Med.* **2001**;7:192–8. doi:10.1038/84643. PMID:11175850.
15. Stacker SA, Caesar C, Baldwin ME, Thornton GE, Williams RA, Prevo R, Jackson DG, Nishikawa S, Kubo H, Achen MG. VEGF-D promotes the metastatic spread of tumor cells via the lymphatics. *Nat Med.* **2001**;7:186–91. doi:10.1038/84635. PMID:11175849.
 16. Dadras SS, Paul T, Bertoncini J, Brown LF, Muzikansky A, Jackson DG, Ellwanger U, Garbe C, Mihm MC, Detmar M. Tumor lymphangiogenesis: A novel prognostic indicator for cutaneous melanoma metastasis and survival. *Am J Pathol.* **2003**;162:1951–60. doi:10.1016/S0002-9440(10)64328-3. PMID:12759251.
 17. Schirotroma C, Cianfrani F, Lacal PM, Odorisio T, Orecchia A, Kani-takis J, D'Atri S, Failla CM, Zambruno G. Vascular endothelial growth factor-C expression correlates with lymph node localization of human melanoma metastases. *Cancer.* **2003 Aug 15**;98(4):789–97. doi:10.1002/cncr.11583.
 18. Mandriota SJ. Vascular endothelial growth factor-C-mediated lymphangiogenesis promotes tumour metastasis. *EMBO J.* **2001**;20:672–82. doi:10.1093/emboj/20.4.672. PMID:11179212.
 19. Rinderknecht M, Detmar M. Tumor lymphangiogenesis and melanoma metastasis. *J Cell Physiol.* **2008**;216:347–54. doi:10.1002/jcp.21494. PMID:18481261.
 20. Christiansen A, Detmar M. Lymphangiogenesis and Cancer. *Genes Cancer.* **2011 Dec**;2(12):1146–58. doi:10.1177/1947601911423028.
 21. Issa A, Le TX, Shoushtari AN, Shields JD, Swartz MA. Vascular endothelial growth factor-C and C-C chemokine receptor 7 in tumor cell-lymphatic cross-talk promote invasive phenotype. *Cancer Res.* **2009**;69:349–57. doi:10.1158/0008-5472.CAN-08-1875. PMID:19118020.
 22. Shields JD, Fleury ME, Yong C, Tomei AA, Randolph GJ, Swartz MA. Autologous chemotaxis as a mechanism of tumor cell homing to lymphatics via interstitial flow and autocrine CCR7 signaling. *Cancer Cell.* **2007**;11:526–38. doi:10.1016/j.ccr.2007.04.020. PMID:17560334.
 23. Shields JD, Emmett MS, Dunn DBA, Joory KD, Sage LM, Rigby H, Mortimer PS, Orlando A, Levick JR, Bates DO. Chemokine-mediated migration of melanoma cells towards lymphatics—a mechanism contributing to metastasis. *Oncogene.* **2007**;26:2997–3005. doi:10.1038/sj.onc.1210114. PMID:17130836.
 24. Shields JD, Kourtis IC, Tomei AA, Roberts JM, Swartz MA. Induction of lymphoidlike stroma and immune escape by tumors that express the chemokine CCL21. *Science.* **2010**;328:749–52. doi:10.1126/science.1185837. PMID:20339029.
 25. Lund AW, Duraes FV, Hirose S, Raghavan VR, Nembrini C, Thomas SN, Issa A, Hugues S, Swartz MA. VEGF-C promotes immune tolerance in B16 melanomas and cross-presentation of tumor antigen by lymph node lymphatics. *Cell Rep.* **2012**;1:191–9. doi:10.1016/j.celrep.2012.01.005. PMID:22832193.
 26. Hirose S, Vokali E, Raghavan VR, Rincon-Restrepo M, Lund AW, Corthésy-Henrioud P, Capotosti F, Halin Winter C, Hugues S, Swartz MA. Steady-state antigen scavenging, cross-presentation, and CD8+ T cell priming: A new role for lymphatic endothelial cells. *J Immunol.* **2014**;192:5002–11. doi:10.4049/jimmunol.1302492. PMID:24795456.
 27. Podgrabska S, Kamalu O, Mayer L, Shimaoka M, Snoeck H, Randolph GJ, Skobe M. Inflamed lymphatic endothelium suppresses dendritic cell maturation and function via Mac-1/ICAM-1-dependent mechanism. *J Immunol.* **2009**;183:1767–79. doi:10.4049/jimmunol.0802167. PMID:19587009.
 28. Swartz MA, Lund AW. Lymphatic and interstitial flow in the tumour microenvironment: linking mechanobiology with immunity. *Nat Rev Cancer.* **2012 Feb 24**;12(3):210–9. doi:10.1038/nrc3186.
 29. Lund AW, Wagner M, Fankhauser M, Steinskog ES, Broggi MA, Spranger S, Gajewski TF, Alitalo K, Eikesdal HP, Wiig H, et al. Lymphatic vessels regulate immune microenvironments in human and murine melanoma. *J Clin Invest.* **2016**;126:3389–402. doi:10.1172/JCI79434. PMID:27525437.
 30. Pastushenko I, Conejero C, Carapeto FJ. Lymphangiogenesis: Implications for Diagnosis, Treatment, and Prognosis in Patients With Melanoma. *Actas Dermo-Sifiligráficas (English Edition).* **2015**;106:7–16. doi:10.1016/j.adengl.2014.11.001.
 31. Dadras SS, Lange-Asschenfeldt B, Velasco P, Nguyen L, Vora A, Muzikansky A, Jahnke K, Hauschild A, Hirakawa S, Mihm MC, et al. Tumor lymphangiogenesis predicts melanoma metastasis to sentinel lymph nodes. *Mod Pathol.* **2005**;18:1232–42. doi:10.1038/modpathol.3800410. PMID:15803182.
 32. Giorgadze TA, Zhang PJ, Pasha T, Coogan PS, Acs G, Elder DE, Xu X. Lymphatic vessel density is significantly increased in melanoma. *J Cutan Pathol.* **2004**;31:672–7. doi:10.1111/j.0303-6987.2004.00249.x. PMID:15491327.
 33. Shields JD, Borsetti M, Rigby H, Harper SJ, Mortimer PS, Levick JR, Orlando A, Bates DO. Lymphatic density and metastatic spread in human malignant melanoma. *Br J Cancer.* **2004**;90:693–700. doi:10.1038/sj.bjc.6601571. PMID:14760386.
 34. Massi D, De Nisi MC, Franchi A, Mourmouras V, Baroni G, Panielo J, Santucci M, Miracco C. Inducible nitric oxide synthase expression in melanoma: implications in lymphangiogenesis. *Mod Pathol.* **2009**;22:21–30. doi:10.1038/modpathol.2008.128. PMID:18660796.
 35. Hirakawa S, Brown LF, Kodama S, Paavonen K, Alitalo K, Detmar M. VEGF-C-induced lymphangiogenesis in sentinel lymph nodes promotes tumor metastasis to distant sites. *Blood.* **2007**;109:1010–7. doi:10.1182/blood-2006-05-021758. PMID:17032920.
 36. Harrell MI, Iritani BM, Ruddell A. Tumor-induced sentinel lymph node lymphangiogenesis and increased lymph flow precede melanoma metastasis. *Am J Pathol.* **2007**;170:774–86. doi:10.2353/ajpath.2007.060761. PMID:17255343.
 37. Cochran AJ, Huang R-R, Lee J, Itakura E, Leong SPL, Essner R. Tumour-induced immune modulation of sentinel lymph nodes. *Nat Rev Immunol.* **2006**;6:659–70. doi:10.1038/nri1919. PMID:16932751.
 38. Pasquali S, van der Ploeg APT, Mocellin S, Stretch JR, Thompson JF, Scolyer RA. Lymphatic biomarkers in primary melanomas as predictors of regional lymph node metastasis and patient outcomes. *Pigment Cell Melanoma Res.* **2013**;26:326–37. doi:10.1111/pcmr.12064. PMID:23298266.
 39. Lund AW, Medler TR, Leachman SA, Coussens LM. Lymphatic Vessels, Inflammation, and Immunity in Skin Cancer. *Cancer Discov.* **2016**;6:22–35. doi:10.1158/2159-8290.CD-15-0023. PMID:26552413.
 40. Stacker SA, Williams SP, Karnezis T, Shayan R, Fox SB, Achen MG. Lymphangiogenesis and lymphatic vessel remodelling in cancer. *Nat Rev Cancer.* **2014**;14:159–72. doi:10.1038/nrc3677. PMID:24561443.
 41. Boone B, Blokx W, De Bacquer D, Lambert J, Ruiter D, Brochez L. The role of VEGF-C staining in predicting regional metastasis in melanoma. *Virchows Arch.* **2008**;453:257–65. doi:10.1007/s00428-008-0641-6. PMID:18679715.
 42. Pastushenko I, Vermeulen PB, Carapeto FJ, Van den Eynden G, Rutten A, Ara M, Dirix LY, Van Laere S. Blood microvessel density, lymphatic microvessel density and lymphatic invasion in predicting melanoma metastases: systematic review and meta-analysis. *Br J Dermatol.* **2014**;170:66–77. doi:10.1111/bjd.12688. PMID:24134623.
 43. Massi D. Tumour lymphangiogenesis is a possible predictor of sentinel lymph node status in cutaneous melanoma: a case-control study. *Journal of Clinical Pathology* **2006**;59:166–73. doi:10.1136/jcp.2005.028431. PMID:16443733.
 44. Tewalt EF, Cohen JN, Rouhani SJ, Guidi CJ, Qiao H, Fahl SP, Conway MR, Bender TP, Tung KS, Vella AT, et al. Lymphatic endothelial cells induce tolerance via PD-L1 and lack of costimulation leading to high-level PD-1 expression on CD8 T cells. *Blood.* **2012 Dec 6**;120(24):4772–82. doi:10.1182/blood-2012-04-427013.
 45. Van der Auwera I, Cao Y, Tille JC, Pepper MS, Jackson DG, Fox SB, Harris AL, Dirix LY, Vermeulen PB. First international consensus on the methodology of lymphangiogenesis quantification in solid human tumours. *Br J Cancer.* **2006 Dec 18**;95(12):1611–25. doi:10.1038/sj.bjc.6603445.
 46. Straume O, Jackson DG, Akslen LA. Independent prognostic impact of lymphatic vessel density and presence of low-grade lymphangiogenesis in cutaneous melanoma. *Clin Cancer Res.* **2003**;9:250–6. PMID:12538477.
 47. Valencak J, Heere-Ress E, Kopp T, Schoppmann SF, Kittler H, Pehamberger H. Selective immunohistochemical staining shows significant prognostic influence of lymphatic and blood vessels in patients with

- malignant melanoma. *Eur J Cancer*. 2004;40:358–64. doi:10.1016/j.ejca.2003.09.009. PMID:14746853.
48. Gannon PO, Poisson AO, Delvoye N, Lapointe R, Mes-Masson A-M, Saad F. Characterization of the intra-prostatic immune cell infiltration in androgen-deprived prostate cancer patients. *J Immunol Methods*. 2009;348:9–17. doi:10.1016/j.jim.2009.06.004. PMID:19552894.
 49. Toader MP, Țăranu T, Toader Ș, Chirana A, Țăranu T. Correlation between lymphatic vessel density and microvessel density in cutaneous malignant melanoma. *Rom J Morphol Embryol*. 2014;55:141–5. PMID:24715179.
 50. Shayan R, Karnezis T, Murali R, Wilmott JS, Ashton MW, Taylor GI, Thompson JF, Hersey P, Achen MG, Scolyer RA, et al. Lymphatic vessel density in primary melanomas predicts sentinel lymph node status and risk of metastasis. *Histopathology*. 2012 Oct;61(4):702–10. doi:10.1111/j.1365-2559.2012.04310.x.
 51. Sahni D, Robson A, Orchard G, Szydlo R, Evans AV, Russell-Jones R. The use of LYVE-1 antibody for detecting lymphatic involvement in patients with malignant melanoma of known sentinel node status. *Journal of Clinical Pathology*. 2005;58:715–21. doi:10.1136/jcp.2004.020123. PMID:15976338.
 52. Tammela T, Alitalo K. Lymphangiogenesis: Molecular mechanisms and future promise. *Cell*. 2010;140:460–76. doi:10.1016/j.cell.2010.01.045. PMID:20178740.
 53. Dieu-Nosjean MC, Giraldo NA, Kaplon H, Germain C, Fridman W-H, Sautès-Fridman C. Tertiary lymphoid structures, drivers of the anti-tumor responses in human cancers. *Immunol Rev*. 2016;271:260–75. doi:10.1111/imr.12405. PMID:27088920.
 54. Avram G, Sánchez-Sendra B, Martín JM, Terrádez L, Ramos D, Monteagudo C. The density and type of MECA-79-positive high endothelial venules correlate with lymphocytic infiltration and tumour regression in primary cutaneous melanoma. *Histopathology*. 2013;63:852–61. doi:10.1111/his.12235. PMID:24102908.
 55. Martinet L, Le Guellec S, Filleron T, Lamant L, Meyer N, Rochemaix P, Garrido I, Girard J-P. High endothelial venules (HEVs) in human melanoma lesions: Major gateways for tumor-infiltrating lymphocytes. *oncoimmunology*. 2012;1:829–39. doi:10.4161/onci.20492. PMID:23162750.
 56. van Baren N, Baurain J-F, Coulie PG. Lymphoid neogenesis in melanoma: What does it tell us?. *Oncoimmunology*. 2013 Jan 1;2(1):e22505. doi:10.4161/onci.22505.
 57. Ladányi A, Sebestyén T, Mohos A, Liskay G, Somlai B, Tóth E, Timar J. Ectopic lymphoid structures in primary cutaneous melanoma. *Pathol Oncol Res*. 2014;20:981–5. doi:10.1007/s12253-014-9784-8. PMID:24781762.
 58. Card CM, Yu SS, Swartz MA. Emerging roles of lymphatic endothelium in regulating adaptive immunity. *J Clin Invest*. 2014;124:943–52. doi:10.1172/JCI73316. PMID:24590280.
 59. Lukacs-Kornek V, Malhotra D, Fletcher AL, Acton SE, Elpek KG, Tayalia P, Collier A-R, Turley SJ. Regulated release of nitric oxide by nonhematopoietic stroma controls expansion of the activated T cell pool in lymph nodes. *Nat Immunol*. 2011;12:1096–104. doi:10.1038/ni.2112. PMID:21926986.
 60. Nörder M, Gutierrez MG, Zicari S, Cervi E, Caruso A, Guzmán CA. Lymph node-derived lymphatic endothelial cells express functional costimulatory molecules and impair dendritic cell-induced allogenic T-cell proliferation. *FASEB J*. 2012;26:2835–46. doi:10.1096/fj.12-205278. PMID:22459150.
 61. Lee E, Pandey NB, Popel AS. Crosstalk between cancer cells and blood endothelial and lymphatic endothelial cells in tumour and organ microenvironment. *Expert Rev Mol Med*. 2015;17:e3. doi:10.1017/erm.2015.2. PMID:25634527.
 62. Ferguson AR, Nichols LA, Zarling AL, Thompson ED, Brinkman CC, Hargadon KM, Bullock TN, Engelhard VH. Strategies and challenges in eliciting immunity to melanoma. *Immunol Rev*. 2008;222:28–42. doi:10.1111/j.1600-065X.2008.00620.x. PMID:18363993.
 63. Fridman W-H, Remark R, Goc J, Giraldo NA, Becht E, Hammond SA, Damotte D, Dieu-Nosjean M-C, Sautès-Fridman C. The immune microenvironment: a major player in human cancers. *Int Arch Allergy Immunol*. 2014;164:13–26. doi:10.1159/000362332. PMID:24852691.
 64. Fridman W-H, Pagès F, Sautès-Fridman C, Galon J. The immune contexture in human tumours: impact on clinical outcome. *Nat Rev Cancer*. 2012;12:298–306. doi:10.1038/nrc3245. PMID:22419253.
 65. Zuckerman NS, Yu H, Simons DL, Bhattacharya N, Carcamo-Cavazos V, Yan N, Dirbas FM, Johnson DL, Schwartz EJ, Lee PP. Altered local and systemic immune profiles underlie lymph node metastasis in breast cancer patients. *Int J Cancer*. 2013;132:2537–47. doi:10.1002/ijc.27933. PMID:23136075.
 66. Spranger S, Gajewski TF. Tumor-intrinsic oncogene pathways mediating immune avoidance. *oncoimmunology*. 2016;5:1–7. doi:10.1080/2162402X.2015.1086862.
 67. Fankhauser M, Broggi MA, Potin L, Bordry N, Jeanbart L, Lund AW, Da Costa E, Hauert S, Rincon-Restrepo M, Tremblay C, et al. Tumor lymphangiogenesis promotes T cell infiltration and potentiates immunotherapy in melanoma. *Sci Transl Med*. 2017 Sep 13;9:eaa4712. doi:10.1126/scitranslmed.aal4712.
 68. Johansson-Percival A, He B, Li Z-J, Kjellén A, Russell K, Li J, Larma I, Ganss R. De novo induction of intratumoral lymphoid structures and vessel normalization enhances immunotherapy in resistant tumors. *Nat Immunol*. 2017;18:1207–17. doi:10.1038/ni.3836. PMID:28892469.
 69. Speiser DE, Liénard D, Rufer N, Rubio-Godoy V, Rimoldi D, Lejeune F, Krieg AM, Cerottini J-C, Romero P. Rapid and strong human CD8+ T cell responses to vaccination with peptide, IFA, and CpG oligodeoxynucleotide 7909. *J Clin Invest*. 2005;115:739–46. doi:10.1172/JCI23373. PMID:15696196.
 70. Baumgaertner P, Jandus C, Rivals J-P, Derré L, Lövgren T, Baitsch L, Guillaume P, Luescher IF, Berthod G, Matter M, et al. Vaccination-induced functional competence of circulating human tumor-specific CD8 T-cells. *Int J Cancer*. 2012;130:2607–17. doi:10.1002/ijc.26297. PMID:21796616.
 71. Kan S, Konishi E, Arita T, Ikemoto C, Takenaka H, Yanagisawa A, Katoh N, Asai J. Podoplanin expression in cancer-associated fibroblasts predicts aggressive behavior in melanoma. *J Cutan Pathol*. 2014;41:561–7. doi:10.1111/cup.12322. PMID:24588302.